2015

Assessment Of Uranium-233 Sample For Nuclear Resonance Fluorescence Measurements

Adrian Beard
North Carolina Agricultural and Technical State University

Assessment of Uranium-233 Sample for Nuclear Resonance Fluorescence Measurements

Adrian Beard

North Carolina A&T State University

A thesis submitted to the graduate faculty

in partial fulfillment of the requirements for the degree of

MASTER OF SCIENCE

Department: Physics

Major: Physics

Major Professor: Dr. Ronald S. Pedroni

Greensboro, North Carolina

2015

The Graduate School
North Carolina Agricultural and Technical State University

This is to certify that the Master's Thesis of

Adrian Beard

has met the thesis requirements of
North Carolina Agricultural and Technical State University

Greensboro, North Carolina
2015

Approved by:

Dr. Ronald S. Pedroni

Major Professor

Dr. Ashot Gasparian

Committee Member

Dr. Abdellah Ahmidouch

Committee Member

Dr. Abdellah Ahmidouch

Department Chair

Dr. Sanjiv Sarin

Dean, The Graduate School

Biographical Sketch

Adrian Beard was born on January 18, 1990, in Pine Bluff, AR. He received the Bachelor of Science degree in Physics from the University of Arkansas at Pine Bluff in 2012. During his college career, he worked as a research scientist for Dr. Mansour Mortizavi, a physicist that advised him at the University of Arkansas at Pine Bluff, doing research under Arkansas Space Grant and was a STEM scholar. Adrian became one of the first scholars under the Louis Stokes Alliance for Minority Participation the year it was established on campus. Adrian Beard was a 2012 initiate of the Gamma Sigma of Kappa Alpha Psi Fraternity Incorporated. Adrian provided service in the public's interest volunteering in community services whenever it was needed. He is a candidate for the Master of Science degree in Physics.

Dedication

I like to dedicate this to mother, father, daughter, family and friends for motivating me throughout my life to stay focused and pursue my dreams. Even in times of struggle and pain I had their support. I give all thanks to them because they didn't have to be in my life but they did. I would like to dedicate this to myself because this is another major accomplishment for me and I have many more to achieve.

Acknowledgments

I would like to thank God for blessing me with all the opportunities and chances to get back up from being knocked down so many times. He has granted me the strength to realize I can do all things through Christ.

I would like to than Dr. Ronald S. Pedroni for all his support and for allowing me the opportunity to be a part of the Triangle University Nuclear Laboratory group. I worked in the lab and saw how it was an honor to be a part of something on the prestigious Duke University campus doing what I love. Through his teaching and collaborations I was able to be the best student I could be. He served as a great adviser to me providing what I needed to make it being 1000 plus miles from home. I would like to thank Dr. Bililign for pushing me to limits I never knew I could reach. The pressure he applied on me to learn mathematics and physics allowed me to be the diamond in the sky I really am. I would like thank Dr. Gasparian for his help in all the many ways he provided, making sure that I was comfortable at the university with fair treatment. I would like to thank Dr. Ahmidouch (Chairperson) for providing the chance to come here and be a graduate student.

I would like to thank Dr. Howell (Director of TUNL), Brent Fallen, and the staff at Duke University for aiding me in understanding and completing my thesis project. Everyone there were great hard working people who provided help whenever it was needed.

I must also give a special thanks to my best friend Cymone Wisemon. Your support and encouragement for the last 5 years of my life enabled me to become a better man. You were the backbone of my success and will forever be until eternity.

Table of Contents

List of Figures

List of Tables

Abstract

The main goals of this work are an assessment of a specific Uranium-233 target to determine if it is suitable for Nuclear Resonance Fluorescence measurements; to advance fundamental nuclear-physics knowledge important for developing the nuclear materials detection capabilities using γ-rays; to provide experimental data needed for building computer models to evaluate concepts of systems for detecting special nuclear materials in cargo containers; and to educate students and young scientists in basic nuclear-physics and the experimental techniques relevant to the mission of the Domestic Nuclear Detection Office (DNDO) at the Department of Homeland Security (DHS).

The Nuclear Resonance Fluorescence (NRF) measurements are carried out at the Triangle Universities Nuclear Laboratory (TUNL) using the High Intensity Gamma-rays Source (HIγS) facility. An assessment of the Uranium-232 contaminant in the sample was made as part of our efforts to measure the radioactive decay and to develop techniques for making NRF measurements on Uranium-233. For the assessment, the energy of the γ-rays emitted from the target without an incident γ-ray beam was measured using high-purity germanium (HPGe) detectors. The collaboration is trying to develop techniques that will help enable NRF measurements of Uranium-233 in addition to other radioactive targets. The nominal energy range covered by the measurements is from 2 to 5 MeV, where the transmission of gamma-rays through steel is close to the maximum value. The overall objectives of the collaboration is to make NRF measurements on actinides.

The work in this thesis is a part of the effort to carry out (γ,γ') measurements on Uranium-233. A substantial goal is to obtain signal above the background signal due to the radioactivity of the sample itself. A sample assaying is an important part of developing

experiments for performing NRF measurements on radioactive samples. In this thesis, the techniques used to assay the radioactive compounds of the Uranium-233 sample is described. What we want to know about our sample is the radioactive decay, can it be used for NRF measurements, its age and how much Uranium-232 contamination is present. In addition a database for the measurements will be created on the TUNL Web site as a national resource for researchers.

CHAPTER 1

Introduction

The goal for this work is to assess the quality of the Uranium-233 sample obtained from Pacific Northwestern National Laboratory (PNNL) for use in nuclear resonance fluorescence measurements. The Domestic Nuclear Detection Office at the Department of Homeland Security is highly interested in developing computer models for evaluating concepts of systems for detecting special nuclear material in cargo containers, especially for shipments across borders into the United States. Experimental data for gamma-ray transitions at energies ranging from 2 to 5 MeV on a variety of nuclei, in particular Actinides are required for gamma-ray beam based detection systems.

1.1 Gamma-Radiation

When French scientist Paul Villard first discovered gamma-radiation in 1900 it became something of great important to science. A radioactive decay known as gamma decay showed that an excited nucleus emits gamma-radiation nearly as soon as it was excited. Villard saw this while studying radium. He soon was able to say that gamma-radiation decays were more powerful than the decays that were previously observed by scientists. Shortly after they were discovered it was determined that gamma-radiation is electromagnetic radiation of high frequency. Meaning the energy of gamma-rays is very high as well. A gamma-ray is considered a photon which is the quantum of light and force carrier. Electromagnetic radiation is a form of energy emitted and absorbed by charged particles that exhibit wave like behavior as it travels through space. The magnetic and electric field components of electromagnetic radiation existed in a fixed ratio of intensity. The two fields both oscillated in phase perpendicular to each other

and perpendicular to the direction of energy and wave propagation. The father of nuclear-physics Ernest Rutherford later gave Villard's discovery its name, Gamma-Ray, in 1903.

1.2 Nuclear Resonance Fluorescence

Nuclear Resonance Fluorescence or resonant photon scattering denotes the process of resonant excitation of nuclear states by absorption of electromagnetic radiation and subsequent decay of these levels by re-emission of the equivalent radiation. Those photons having the right energy will excite a target nucleus with a certain probability. The probability can be expressed by the ground state transition width, which is related to the transition strength and to the transition matrix elements. After a very short time the excited nuclei will decay either back to the ground state or to some other lower energy excited state by emitting gamma-rays.

Gamma-rays collide with the nucleus putting the nuclear system as a quantum mechanical ensemble in a state where the energy is high. Now the nucleus has to decay to the ground state by releasing high energy photons at discrete energies that can be detected and processed into graphs or histograms using electronics and computer programs. NRF can be quantified during gamma-ray spectroscopy which just shows the energy spectra produced by the sample at different energies and intensities. Something to keep in mind about NRF experiments is that as the energy of incident photons increases, the average spacing between nuclear energy levels descends. This means that the average spacing between energies may be lower than the width of each NRF resonance. Determination cannot be analytical and must rely on special applications like signal processing.

Nuclear Resonance Fluorescence is an excellent method with which to probe low-lying dipoles excitations in nuclei because of the extremely high selectivity of real photons, in exciting such states. This selectivity stems from the small momentum transfer of real photons, in contrast

to virtual photons from electron scattering experiments. The development in recent years of high-efficiency germanium detectors with excellent energy resolution, in conjunction with high-intensity photon beams, has provided the necessary tools to study the fine structure of magnetic and electric dipole strength distributions in detail. The fundamental advantage of the photon scattering technique is that the electromagnetic interaction mechanism is the best-understood interaction in all of science. This understanding allows one to extract detailed information about the structure of nuclei and the transitions between different nuclear states in a completely model independent way. Thus results from these kinds of experiments are as robust as any results of nuclear science.

An NRF facility was established at TUNL to address some of the most fundamental questions of nuclear structure at low excitation energies. This facility, for example, allows one to probe the transitions between three major shapes of nuclei; spherical nuclei, quadrupole-deformed nuclei, and tri-axial nuclei. The proposed studies will investigate the distribution of magnetic and electric transitions strengths, and thus, provide rigorous tests and guidance to theoretical models. Basic data following from application of this technique can also be used for practical purposes such as hazardous waste assay and imaging. A simplified scheme of an NRF experiment is shown in Figure 1.1.

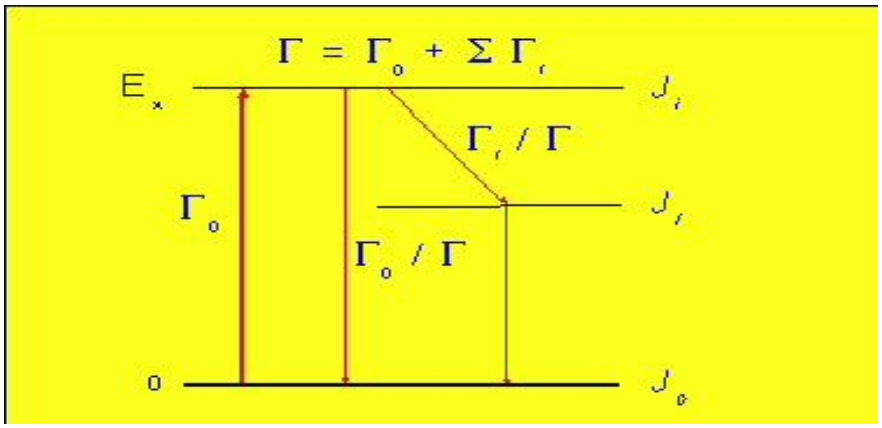

Figure 1.1 NRF Experiment Schematic

The NRF method is used for study of low multi-polarity transitions with large partial widths to the ground state. This means that the photon has a small probability to transfer angular momentum to the atomic nucleus. Due to its low detection limit it represents an outstanding tool for the examination of dipole transitions. The photon scattering cross section depends on the branching ratio of the excited level to ground state. The energies E_x of the excited states, their lifetimes τ, their angular momenta J and their parities π provide important information about the nuclear structure.

The use of quasi mono-energetic, easily energy tunable, and 100% linear polarized gamma beams allows the measurement of excitation energies, spin, parities, decay branching ratios, ground-state transition widths, and hence the reduced excitation probabilities in a completely model-independent way. On the other hand, this experimental information is not easy to measure with photon scattering experiments using unpolarized bremsstrahlung beams. Hence, using the advantages of the gamma-ray source at the High Intensity Gamma-ray Source (HIγS) facility at the Triangle Universities Nuclear Laboratory will allow us to measure systematically the photo absorption and subsequent dexcitation of nuclei.

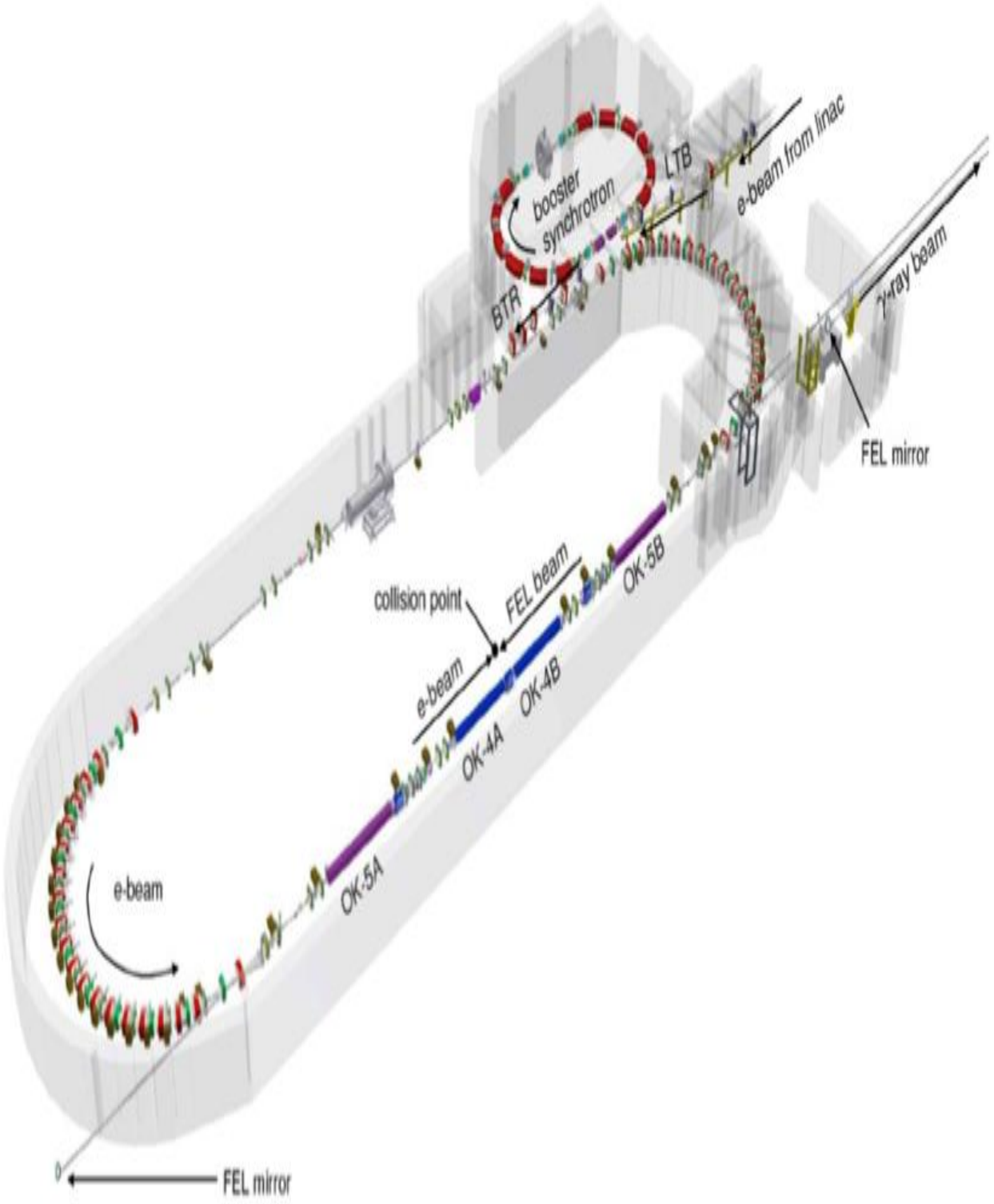

Figure 1.2 High Intensity Gamma-ray Source Facility

1.3 HIγS Facility

A schematic of the High Intensity Gamma-ray Source facility is shown in *Figure 1.2* below. HIγS is the most intense accelerator-driven gamma-ray source in the world because of its characteristics. It has a 1.2 GeV storage ring free electron laser (FEL) with an energy acceptance of $\pm 3.5\%$ and a total revolution frequency of 2.7898 MHz. The total beam flux before collimation is 10^8 gammas per second. Bunch lengths range from 30-120 ps and a maximum single bunch current with a range of 50 mA to 95 mA with lasing, a typical two bunch current that is limited by the free electron laser mirror in the range of 60 – 80 mA. The free electron laser mirror has a Gaussian peak approximately at 450 nm, but on both sides of the peak maximum lasing can occur at approximately 430 nm. HIγS is operated by the staff and researchers at the Triangle Universities Nuclear Laboratory (TUNL) at Duke University along with University of North Carolina at Chapel Hill, North Carolina State University and the rest of the affiliated institutions in the country. The linear and circular polarized beams are what makes HIγS ideal for making NRF measurements. Compton Back-Scattering is the interaction that takes place with HIγS. What happens is an electron is emitted around the electron storage ring while a photon is emitted in the lasing cavity (wiggler magnets). The photon back-scatters off the free electron laser mirror in perfect timing with the electron so they can collide. Once the photon and electron collide, energy is transferred from the electron to the photon.

1.4 Uranium-233

Uranium is a chemical element of the periodic table in the actinide category with atomic number 92 specifying the number of protons and electrons. Uranium has several isotopes (Uranium-232, 233, 235, and 238) that are radioactive and are of interest for NRF measurements.

For this work, the isotope, Uranium-233, was assessed for its suitability as a target for Nuclear Resonance Fluorescence measurements.

Uranium-233 is transmuted from Thorium-232 in a reactor during the Thorium Fuel Cycle which is a nuclear fuel cycle that uses the naturally abundant isotope of Thorium, Thorium-232.

Figure 1.3 Natural Uranium

Thorium-232 will breed Thorium-233 via neutron capture in the reactor once Thorium-233 is formed it is followed by two sequential beta decays that produce Uranium-233.

$$\mathrm{n} + {}^{232}_{90}Th \rightarrow {}^{233}_{90}Th \xrightarrow{\beta} {}^{233}_{91}Pa \xrightarrow{\beta} {}^{233}_{92}U \qquad (1.1)$$

The main challenge in making (γ,γ) measurements on Uranium-233 is that all Uranium-233 target materials contain trace amounts of Uranium-232, that is a prolific emitter of gamma-rays even for small amounts because of its relatively short half-life of about 69 years. Due to the isotope being so radioactive and hot from the kinetic energy given off as heat because of the short half-life it cannot be handled unless proper radiation safety procedures are in effect.

Production of Uranium-233 invariably produces small amounts of Uranium-232 as an impurity because of parasitic (n,2n) reactions on Uranium-233 itself.

As previously stated, the Department of Homeland Security's Domestic Nuclear Detection Office is interested in knowing the excited energy levels of Uranium-233 (along with other nuclei).

1.5 Online Database for Nuclear Resonance Fluorescence Data

In the middle of the research, the author of this work was given the additional project of developing a comprehensive database for NRF measurements. This database will serve as a national resource for researchers conducting work in applied and basic science areas that use NRF data. The database will be accessible online from the TUNL website. The DNDO/ARI program managers recommended that such a database be created, and it is a natural extension of our ongoing literature studies of NRF measurements used to develop new experiments. Dr. Howell, director of TUNL, assigned this author the project to include in the body of this work. The database took long months of literature reviews of (γ,γ) reaction papers to find every possible experiment done. Of all the isotopes that were found, many had most of the data that was expected. On the Brookhaven National Laboratory website there were publications that had to be read to determine if they of interest to the DNDO overall project.

The chapters to follow describe the experimental techniques used in the attempt to perform NRF measurements on the Uranium-233 sample, the method used to assay the sample and the online databased of NRF cross-section measurements.

CHAPTER 2

Nuclear Resonance Fluorescence Attempt

In this chapter the experimental setup for the first attempt to carry out NRF on our Uranium-233 target will be discussed.

2.1 Target Room Setup

The existing HIGS target room is called the Gamma-Vault. The area of the Gamma-vault is approximately 900 square-feet. The beam passes along the center of the room at a height of approximately 72 inches from the floor. The Gamma-vault has a removable wall for access during installation and removal of large experimental equipment. The room has utilities for compressed air, compressed nitrogen, and de-ionized water. The room also has electrical connections for 115 V, 220 V, and 408 V (with three phases). The Gamma-vault has an overhead crane with one axis and capacity of 3 tons. There is also a smaller lift available for loads up to 1000 lbs.

There is a smaller target room called upstream target room (UTR, 21 feet long along the beam direction, 12 feet wide, and beam height of approximately 49.5 inches) that is also available for a majority of the experiments running below 20 MeV of gamma-ray energy. The UTR has stands for a number of HPGe detectors, includes beam imagery, and a large HPGe detector for beam monitoring. The UTR has a rolling door for placement or removal of large size objects.

There are two main types of detectors, scintillation detector and semiconductor detector. The main difference between an insulator and a semiconductor is in the size of the energy gap, which can perhaps be 5 eV in an insulator and 1 eV in a semiconductor. The detector that was used to take the assay of the Uranium-233 was a 60% High-purity Geranium because it is

recommended better to use when ionizing radiation detection to measure the effect of incident charged particles or photons. 1 out of every 10^9 electron's at room is thermally excited across the gap and into the conduction band, leaving a valence band vacancy known as the hole. Dopants are added to control electrical conduction in the semiconductors. The number of hole-pairs is proportional to radiation energy of the semiconductor detector. The detector was cooled down with liquid nitrogen to keep it cold throughout the experiment. The charge carriers are all positively charged holes because they are above the valence band. The 60% High-purity Geranium detector was place a distance of 245 centimeters in length and 93 centimeters in height from the sample of Uranium-233. The Uranium-233 was in a stainless steel holder that was an inch in diameter and depth.

Figure 2.1 Holder that the sample was placed in.

The energy calibration sources that were used for this experiment were Cesium-137, Europium-152 and Cobalt-60. The gamma-ray energy from the Cesium-137 was 661.657 keV, gamma-ray energy from Europium-152 was 1408 keV and gamma-ray energy from Cobalt-60

was 1332 keV. Two experimental runs, run number 646 and number 647, were performed on the Uranium-233 target. The description of run number 646 had an energy calibration with the Cesium-137 and Cobalt-60. The description of the run number 647 was for the data accumulation for Uranium-233 target. The measurement was done in the Upstream Target Room in the High Intensity Gamma-ray Source facility using the Genie Data Acquisition Software system that is all engineered by the

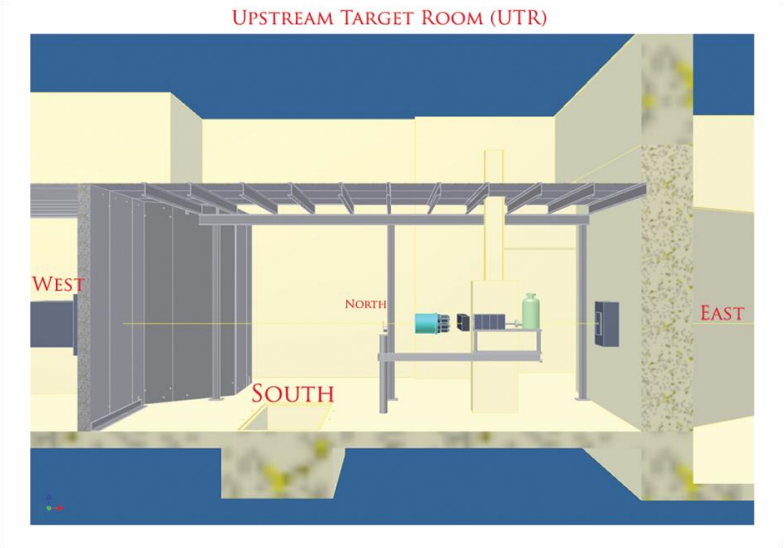

Figure 2.2 Upstream Target Room (UTR)

Technicians of the High Intensity Gamma-ray Source facility.

2.2 Interaction with Matter by Gamma-rays

The three primary processes of how gamma-rays interact with matter where given previously. They were photoelectric effect, Compton Scattering and pair production. The only one that plays a part in this work is Compton Scattering, Compton Back-Scattering, to be exact.

Compton Scattering is the processing by which a photon scatters from a nearly free atomic electron, resulting in a less energetic photon and a scattered electron carrying the energy lost by the photon. It is an inelastic scattering because the wavelength of the scattered light is different from the incident radiation. The origin of the effect can be considered as an elastic collision between a photon and an electron was very much larger than the binding energy of the atomic electron. Binding energy is the mechanical energy required to disassemble a whole into separate parts. Gamma-ray energy in energy from Gamma-ray for theta equals zero degrees.

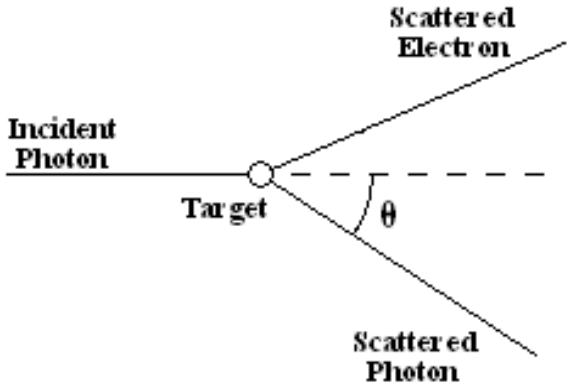

Figure 2.3. The geometry of Compton scattering

Geometry has to be used in order to find the probability for Compton scattering at an angle theta taking a differential cross section over some solid angle.

2.3 Detector

The two types of detection where discussed previously but briefly just describing the difference in the two. As stated before the 60% High-purity Geranium detector was used for the measurement on the Uranium-233. The detector which has valence-4 atoms form four covalent bonds with neighboring atoms due to it being form from solid crystal. All valence electrons thus

participate in covalent bonds, and the band structure shows a filled valence band and an empty conduction band. To control the electrical conduction in semiconductors, small amounts of materials called dopants are added. Atoms are introduced into the lattice with valence 3 or 5 when doping.

Fabrication procedure for High-purity Geranium detectors is begun with a sample of p-type material and diffused in its surface a concentration of Li atoms, which tent to form donor states and thereby created a thin n-type region. Under reverse bias and at a slightly elevated temperature, the Li drifts in the p-type region, making quite a large depletion region. Such detectors are known as lithium-drifted Ge and Si detectors. The reason the detector was kept cool is because it reduces the thermal excitation of electrons across the energy gap, thereby reducing the background electrical noise produced by the detector. High-purity Geranium detectors have large volumes, owing to advances in the techniques of refining Geranium crystals. It has to be at a low temperature of 77 kelvins to keep down the background noise.

Figure 2.4. High-purity Geranium Detector.

2.4 NRF

The NRF measurement was done by allowing the target to sit in front of the four HPGe detectors in the target room in front of the beam. Without any beam turned on the Uranium-233 sample gave off huge amounts of radiation in the form of gammas. The energy transitions were recorded for a four hours and the analysis resonances peaks of the excitation energy given off from the sample. Once the time of flight was over the transition energies were viewed in a signal processing software Gaussian fit to calculate the number of counts. The number of counts tells us the area of the peak at that discrete energy on the spectrum.

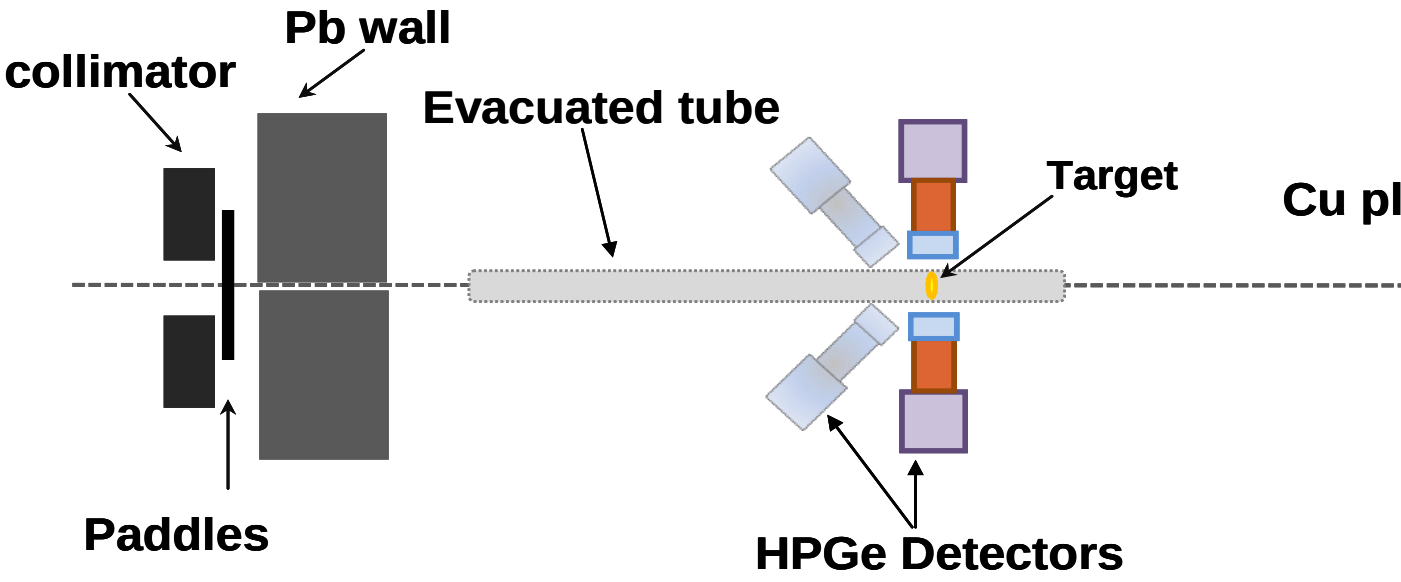

Figure 2.5 Schematic of the HPGe Detectors for the NRF measurement

The NRF measurement was analyzed to determine what isotopes give off those excitation energies in the spectrum. The gamma-ray that was most active was the 2614 MeV gamma in the spectrum. Next was to determine whether the gamma-ray came from the Uranium-233 or its contaminant Uranium-232. Looking on the TUNL website's nuclear database of excitation energies for specific isotopes, what was discovered was that the 2614 MeV gamma-ray come from Thallium-208. Thallium 208 is in the alpha decay chain of Uranium-232. From this what the conclusion gives no excitation energies coming from Uranium-233 were detectable. The activity of the contaminant Uranium-232 is all that is detected in the measurement.

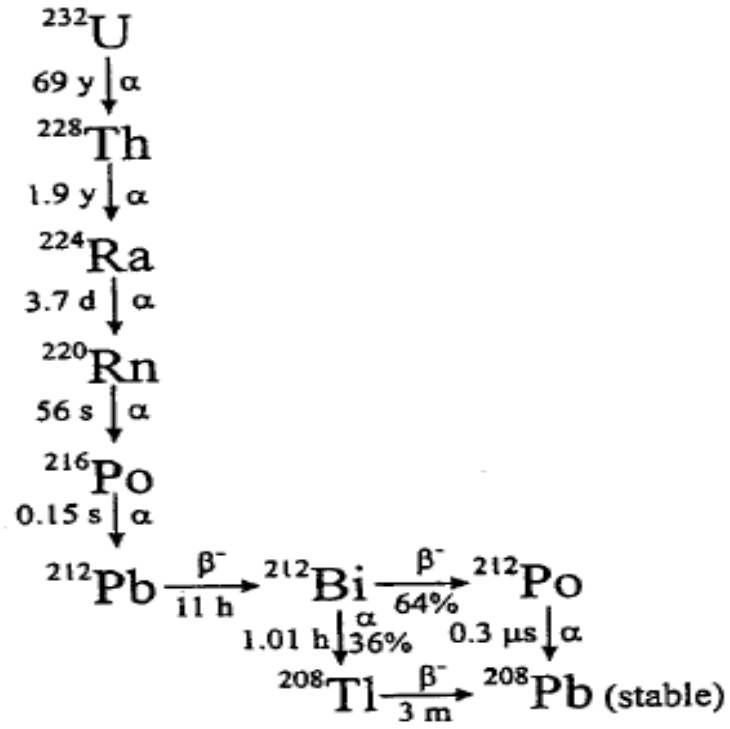

Figure 2.6 Decay Chain of Uranium-233

The histogram of energy versus time of Flight showed the most troublesome gamma-ray that it emitted in the decay chain at an energy of 2614 keV and comes from the decay of the first

excited stated in Thallium-208 to the ground state Lead-208. That short half-life that Uranium-232 has allows the determinations of it emitting that gamma-ray. The histogram illustrates that the dominant feature in the detected gamma-ray energy spectrum is the 2614 keV gamma-ray from the decay of Uranium-232.

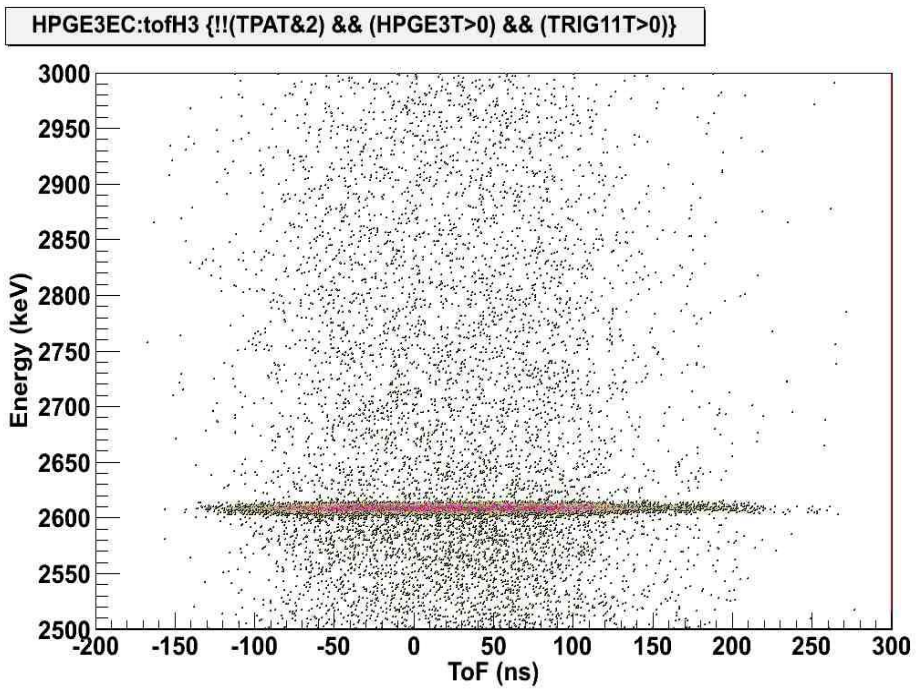

Figure 2.7 Histogram of the 2614 eV gamma emitted from the NRF measurement

The Pacific Northwestern National Laboratory specified that there is 16 milligrams of Uranium-232 with a specific activity was 27 mCi and that there are 4 grams of Uranium-233 with specific activity was 38.6 mCi. These where just specifications made before the measurement by the Pacific Northwestern National Laboratory in the inventory of targets paper work. This knowledge of the sample was quickly concluded that the trace amount of Uranium-232 would give a contamination level that may be too high to make a NRF measurement. A more

pure sample would be needed but attempts to check the purity were still made before search for a better sample. The isotopic ratio would be several hundred parts per million. The attempts to make NRF measurements on Uranium-233 where unsuccessful because we could not get signals above the background noise. In the next chapter the assessment on the Uranium-233 will be discussed in detail since the attempt to make an NRF measurement seemed impossible due to the trace amounts of Uranium-232.

CHAPTER 3

Assay of the Urainium-233 Target

In this chapter, the actual work done to make the assay of the Uranium-233 target will be discussed. The radioactive decays of Uranium-233 and Urainium-232 will be explained. The gamma-ray spectroscopy measurements will also be discussed as well as the calculations performed to determine the actual amount of Urainium-232 in the Uriainium-233 target. The final results will be given with our conclusion about the suitability of the target for NRF measurements.

The target room was properly checked by the technicians that operate the lab daily. Since all measurements were done at night we made sure of this early enough every time. The detector was properly placed and determined to be fine. The sample was held with radiation precautions like the radiation safety training has always recommended. Once everything was put into place, data collection started.

3.1 Data Collection Process

The data collection takes some time before we start because only a certain characteristic can be given attention during each measurement. You can't measure the isotopes unless you know what specific states are known. The detector and cables have to be properly shielded to avoid the background noises that occur during the data collection. The detector was in the horizontal plane and was used to monitor the flux. The reason the detector was shielded is because that background noise can affect the collection process. Loud noise can be the transition frequency that you are seeing on the Data Acquisition system so you have to be careful of that. To avoid it aluminum and lead was wrapped around the detectors to cover up some of that background noise. An oscilloscope was used to test the resonances that had high voltage

amplitudes. The aim is to get the amplitudes under 10 millivolts or as close to being grounded as possible.

The energy spectra needed enough time to grow high enough to show lines above the background noise. Once that occurred you could see the actual energy arising from the noise. Too much background noise can mess up the resolution of the graph or histogram when looking at the transitions. Determining the sources from the actual target is not a hard task because all the energies at of the sources are well known. The sources where placed by the detector as always for their contributions. The measurement time was at 1:50 a.m. It lasted until 7:30 a.m.

3.2 Data Acquisition of the Radioactive Decay

What the Data Acquisition system does is process the sampling signals that measure real world physical conditions and converting the resulting samples into digital numeric values that can be manipulated by a computer. It typically converts analog wave-forms into digital values for processing. The components of the data acquisition system include sensors that convert physical parameters to electrical signals, signal conditions circuitry to convert sensor signals into a form that can be converted to digital values, and analog to digital converters, which converts conditioned sensor signals to digital values. Pascal, FORTRAN, and many other programing languages are used to develop the l software for the data acquisitions.

When measuring the radioactive decay of substances such as isotopes certain laws hold that researcher needs to be familiar with. The activity of radioactive isotopes is based on two factors: the quantity of the isotope present and the half-life of the isotope. The calculations of the activity with precision of the calculated isotope at any given time and direct calculation of the radioactivity is being measured in this experiment. The propagation of uncertainty in the activity due to the uncertainties in the isotope data is quantified through a Monte Carlo method.

The half-lives of isotopes span many orders of magnitude, from short-lived isotopes that decay nearly instantaneously to relatively stable isotopes with very long half-lives. Because of the large range of half-lives, calculation the quantity of each isotope present in a given decay chain after a period of time may be difficult due to the tough approach needed to be taken because of the differential equations describing radioactive decay. These equations are known as the Bateman equations, which we do not do by hand. Computer software is relied on for this matter. To avoid this stiffness, solutions are most commonly found by making approximations. In this typical implementation, isotopes are evaluated differently based on the magnitude of the half-life in relation to other isotopes in the chain and the position of the isotope in the chain (the first isotope in the chain versus an isotope near the end of the chain).

For some applications, models find gamma-ray activity by using an approximation that the gamma-ray activity decays as $t^{-1.2}$. This approximation is used for any arbitrary gamma-ray energy range as well as total activity. The new model seeks to improve upon this approximation by calculating the activity directly for each time step for any given energy bin. A more robust method of calculating radioactive decays is desired to increase the precision of the results. A method which treats all isotopes the same, regardless of position in the chain or relative magnitude, will treat decay chains uniformly and therefore more predictably and with greater precision. It is important to know the quantities of each isotope remaining after a given time more precisely than available with current methods. This will allow for more precise calculation of the activity of the radioactive isotopes and lead to a better understanding of high energy gamma-rays emitted following the neutron induced fission of uranium isotopes.

The decay rate of a radioactive substance was found to decrease exponentially with time. Radioactive decay was found to follow a statistical law, that is, it is impossible to predict when any give atom will disintegrate. The rate at which a radioactive substance N decays is given by

$$\frac{dN}{dt} = -\lambda N \tag{3.1}$$

Where N is the number of radioactive atoms and λ is called the decay constant, which represents the probability per unit time for one atom to decay. The fundamental assumption in the statistical law for radioactive decay is that this probability for decay is constant, that is, it does not depend on time or on the number of radioactive atoms present. Equation 3.1 can be integrated with the boundary condition that the initial number of radioactive atoms is $N_0 = N(0)$. This leads to the exponential law of radioactive decay

$$N = N_0 e^{-\lambda t} \tag{3.2}$$

For measurement purposes, it is often convenient to express Equation 3.2 in terms of activity A of a radioactive substance, which is defined to be the number of decays per unit time or simply $A = \lambda N$. If we multiply both sides of Equation 3.2 by λ, we find that

$$\lambda N = \lambda N_0 e^{-\lambda t} \tag{3.3}$$

It follows that

$$A = A_0 e^{-\lambda t} \tag{3.4}$$

were A_0 is the initial activity of the radioactive substance. The unit most commonly used in activity measurement is the curie (Ci), which is defined as 3.7×10^{10} decays per second.

The half-life of a radioactive substance is defined as the elapsed time over which the radioactive substance has decreased to half its original abundance. Thus, by letting $N = N_0/2$ in Equation 3.2, the half-life is given by

$$\tau_{\frac{1}{2}} = \frac{ln2}{\lambda} \tag{3.5}$$

The mean life, t, or the average amount of time a radioactive element lives, is given by

$$t = \frac{1}{\lambda} \tag{3.6}$$

Thus, the mean life is simply the inverse of the decay constant. During the mean life, the abundance of a radioactive substance decreases by a factor of 1/e.

3.3 Assay of Uranium-233

During the NRF attempt on Uranium-233 the trace amounts of Uranium-232 came into effect due to its short half-life of about 69 years. The radiation it gives off creates a lot of heat which is kinetic energy. Our target, which was obtained from the Pacific Northwestern National Laboratory, is specified to consist of 4.0 grams of Uranium-233 and 16 milligrams of Uranium-232 which would be 4000 ppm of Uranium-232 contamination.

In searching for a clearer Uranium-233 sample with mass of a few grams, we found that the National Isotope Development Center has such samples with down to about 200 ppm of Uranium-232 contaminant. Before obtaining a new sample, the specifications that were provided by the Pacific Northwestern National Laboratory needed to be verified using gamma-ray spectroscopy techniques to assay the sample. The assay was set up by placing the Uranium-233 target 245 centimeter in length from the detector and 93 centimeter from the ground. There was only one HPGe used for the assay. Assaying techniques were based on assuming that the mass

specification for Uranium-233 is correct and that all the radioactive nuclei used came from the decay of either directly or indirectly solely from the decay of either Uranium-233 or Uranium-232. The mass given from the Pacific Northwestern National Laboratory was 4 grams for the Uranium-233. So the activity was checked using a simple Specific Activity formula:

$$S_A = \frac{ln2 \cdot N_A}{\tau_{\frac{1}{2}} \cdot M} \tag{3.7}$$

N_A is Avogadro's number which is 6.0221413×10^{23} nuclei or molecules per mol., $\tau_{\frac{1}{2}}$ is the half-life of the Uranium-233 and M is the mass or molar mass of the isotope. The Specific Activity for Urainium-233 was calculated to be 38.5 millicurie which matched 38.54 millicurie quoted by PNNL. The Specific Activity was also calculated for the 16 milligrams of Uranium-232 resulting in a value of 357.6 microcurie. The calculated activity of the Uranium-232 was far larger than that quoted by PNNL. The Pacific Northwestern National Laboratory was called to see if they could explain the difference in the activity for Urainium-232. The age of the sample came into question, and the Pacific Northwestern National Laboratory did not know the actual age but gave an estimate of maybe 30 to 40 years old.

The age of the sample was determined by measuring the decay rates of Francium-221 and Bismuth-213. The ratio of the number of nuclei was used in both these isotopes. The number of nuclei in the Uranium-233 was calculated to be $1.033819742 \times 10^{22}$ from a simple formula:

$$m = MN/N_A \tag{3.8}$$

Solving for N, which is the number of nuclei gives:

$$N = m N_A/M \qquad (3.9)$$

N_A, being Avogadro's number, M, being the molar mass of the isotope and m being the amount of the Uranium-233 in grams. Having this number of nuclei for the parent nucleus and plotting the number of nuclei versus time in years, a graph is developed. A gamma-ray spectroscopy technique was used to determine the age of the sample. The key was to not allow the daughter isotopes come into equilibrium. Well Francium-221 and Bismuth-213 abundances have not reach equilibrium and their decay produce gamma-ray lines that are prominent in the gamma-ray energy spectrum.

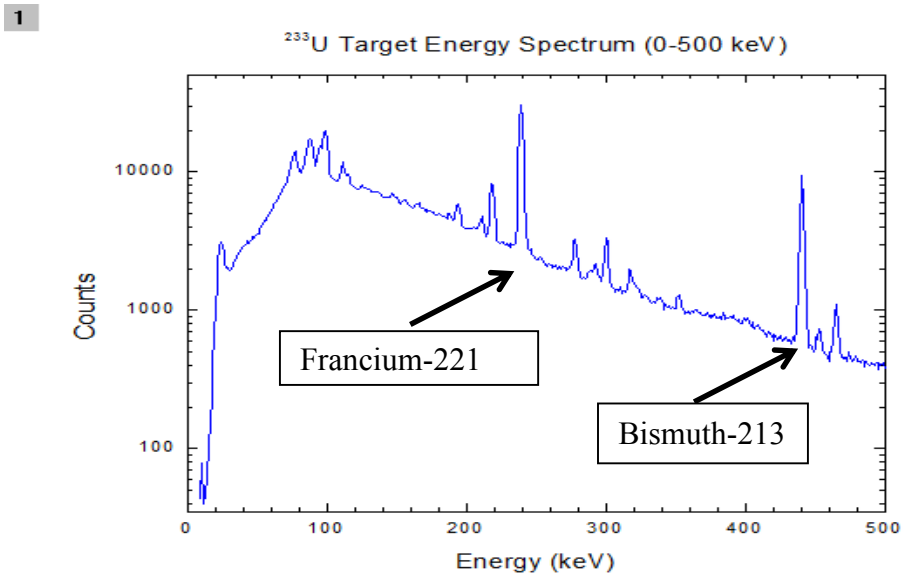

Figure 3.1. Energy Spectrum showing Francium-221 and Bismuth-213

The sample was determined to be about 37 years old which implies that the abundance of the Thallium-208 produced in the decay of Uranium-232 is in equilibrium. Definition of the decay constant and number of nuclei bring proportional says that a parent nuclei decays equally to the daughter nuclei when in equilibrium.

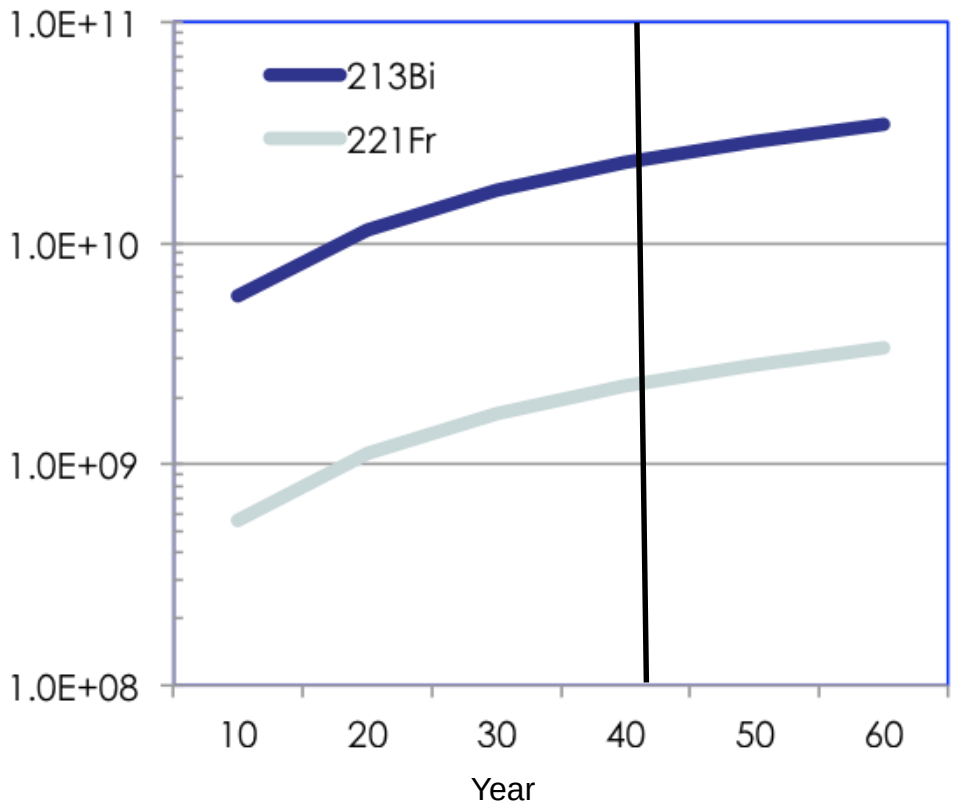

Figure 3.2. Number of Nuclei versus number of years of daughter nuclei not in equilibrium

$$N_p\lambda_P = N_d\lambda_d \tag{3.10}$$

N_p being the number of nuclei of the parents nuclei, λ_P being the decay constant of the parent nuclei, N_d being the number of nuclei and λ_d being the decay constant of the daughter.

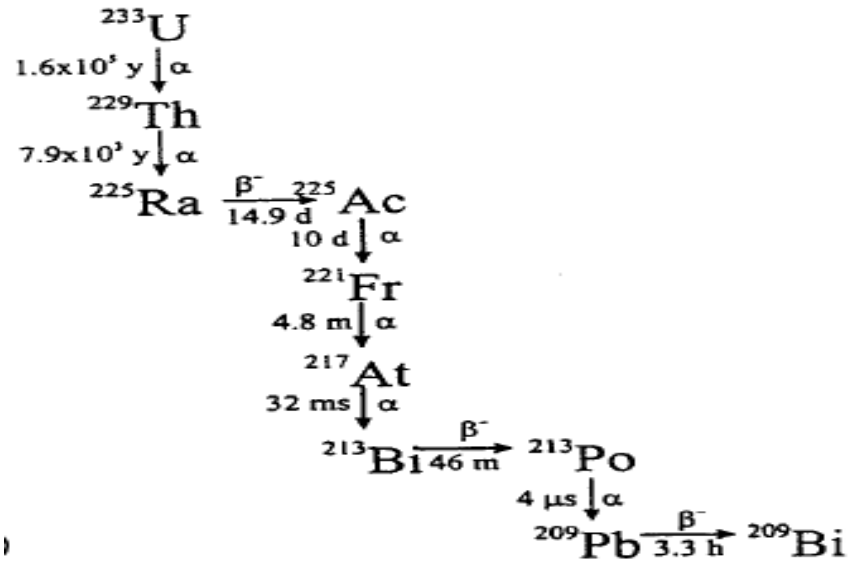

Figure 3.3. Decay Chain of Uranium-233.

Knowing this tells us that the gamma-ray energy at 2614 was the beta decay of the Thallium-208. Theoretical and statistical proof from the Triangle University Nuclear Laboratory says this as well:

Table 3.1 Characteristics of Thallium-208

Parent Nucleus	Parent E(level)	Parent Jπ	Parent $T_{1/2}$	Decay Mode	GS-GS Q-value (keV)	Daughter Nucleus	Decay Scheme	ENSDF file
$^{208}_{81}$Tl	0.0	5+	3.053 m *4*	β⁻: 100 %	4999.0 *17*	$^{208}_{82}$Pb		

Beta-:

Energy (keV)	End-point energy (keV)	Intensity (%)	Dose (MeV/Bq-s)
154.43 *59*	518.5 *17*	0.052 % *5*	8.0E-5 *8*
187.88 *61*	616.1 *17*	0.017 % *5*	3.2E-5 *9*
196.43 *60*	640.6 *17*	0.044 % *5*	8.6E-5 *10*

208.79 *62*	675.6 *17*	0.0050 % *20*	1.0E-5 *4*
218.44 *62*	702.7 *17*	0.101 % *21*	2.2E-4 *5*
230.73 *67*	737.0 *18*	0.0020 % *10*	4.6E-6 *23*
260.44 *63*	818.6 *17*	0.227 % *9*	5.91E-4 *23*
280.78 *64*	873.7 *17*	0.175 % *23*	4.9E-4 *6*
329.64 *68*	1003.4 *18*	0.007 % *3*	2.3E-5 *10*
342.90 *66*	1038.1 *17*	3.18 % *6*	0.01090 *21*
348.43 *66*	1052.6 *17*	0.046 % *3*	1.60E-4 *10*
358.70 *66*	1079.2 *17*	0.63 % *5*	0.00226 *18*
441.53 *68*	1290.6 *17*	24.2 % *3*	0.1069 *13*
535.39 *70*	1523.9 *17*	22.2 % *5*	0.119 *3*
649.48 *71*	1801.3 *17*	49.1 % 7	0.319 *5*

Mean beta- energy: 560 keV *7*, total beta- intensity: 100.0 % *9*, mean beta- dose: 0.559 MeV/Bq-s *9*

Electrons:

Energy (keV)	Intensity (%)	Dose (MeV/Bq-s)
Auger L 7.97	4.50 % *13*	3.59E-4 *11*
Auger K 56.7	0.27 % *3*	1.52E-4 *17*
CE K 123.40 *15*	0.166 % *10*	2.05E-4 *12*
CE K 145.36 *15*	0.170 % *18*	2.5E-4 *3*
CE K 164.61 *10*	0.40 % *3*	6.5E-4 *4*
CE K 189.367 *5*	2.88 % *14*	0.0054 *3*
CE L 195.54 *15*	0.0285 % *16*	5.6E-5 *3*
CE M 207.55 *15*	0.0067 % *4*	1.39E-5 *8*
CE N 210.51 *15*	0.00170 % *10*	3.58E-6 *21*
CE O 211.32 *15*	3.38E-4 % *20*	7.2E-7 *4*
CE P 211.40 *15*	3.62E-5 % *21*	7.6E-8 *4*
CE L 217.50 *15*	0.036 % *4*	7.8E-5 *8*
CE M 229.51 *15*	0.0086 % *9*	1.97E-5 *21*
CE N 232.47 *15*	0.00218 % *23*	5.1E-6 *5*
CE O 233.28 *15*	4.3E-4 % *4*	9.9E-7 *10*
CE P 233.36 *15*	4.0E-5 % *4*	9.4E-8 *10*
CE L 236.75 *10*	0.0734 % *24*	1.74E-4 *6*
CE M 248.76 *10*	0.0173 % *5*	4.31E-5 *14*
CE N 251.72 *10*	0.00441 % *14*	1.11E-5 *3*
CE O 252.53 *10*	8.7E-4 % *3*	2.20E-6 *7*
CE P 252.61 *10*	9.0E-5 % *5*	2.27E-7 *11*
CE L 261.510 *5*	0.492 % *23*	0.00129 *6*
CE M 273.520 *5*	0.115 % *5*	3.15E-4 *15*
CE N 276.477 *5*	0.0292 % *14*	8.1E-5 *4*
CE O 277.296 *5*	0.0058 % *3*	1.62E-5 *8*
CE P 277.370 *5*	6.2E-4 % *3*	1.73E-6 *8*

CE K	422.77 *10*	1.90 % *3*	0.00804 *14*
CE L	494.91 *10*	0.321 % *6*	0.00159 *3*
CE K	495.1825 *21*	1.284 % *19*	0.00636 *10*
CE M	506.92 *10*	0.0750 % *13*	3.80E-4 *7*
CE N	509.88 *10*	0.0190 % *3*	9.70E-5 *17*
CE O	510.69 *10*	0.00380 % *7*	1.94E-5 *3*
CE P	510.77 *10*	4.07E-4 % *8*	2.08E-6 *4*
CE L	567.3262 *21*	0.349 % *5*	0.00198 *3*
CE M	579.3363 *21*	0.0859 % *13*	4.97E-4 *8*
CE N	582.2934 *21*	0.0218 % *3*	1.267E-4 *20*
CE O	583.1118 *20*	0.00415 % *6*	2.42E-5 *4*
CE P	583.1855 *20*	3.44E-4 % *5*	2.01E-6 *3*
CE K	634.04 *12*	0.0077 % *13*	4.9E-5 *8*
CE L	706.18 *12*	0.00129 % *22*	9.1E-6 *15*
CE M	718.19 *12*	3.0E-4 % *5*	2.2E-6 *4*
CE N	721.15 *12*	7.7E-5 % *13*	5.5E-7 *9*
CE O	721.96 *12*	1.5E-5 % *3*	1.11E-7 *19*
CE P	722.04 *12*	1.6E-6 % *3*	1.18E-8 *20*
CE K	772.552 *4*	0.271 % *4*	0.00210 *3*
CE L	844.696 *4*	0.0450 % *7*	3.80E-4 *6*
CE M	856.706 *4*	0.01049 % *17*	8.98E-5 *15*
CE N	859.663 *4*	0.00266 % *4*	2.29E-5 *4*
CE O	860.482 *4*	5.33E-4 % *9*	4.58E-6 *7*
CE P	860.555 *4*	5.71E-5 % *10*	4.92E-7 *8*
CE K	2526.507 *10*	0.1708 % *24*	0.00431 *6*
CE L	2598.650 *10*	0.0292 % *5*	7.60E-4 *13*
CE M	2610.660 *10*	0.00685 % *10*	1.79E-4 *3*
CE N	2613.617 *10*	0.001739 % *25*	4.54E-5 *7*
CE O	2614.436 *10*	3.45E-4 % *5*	9.02E-6 *13*
CE P	2614.510 *10*	3.61E-5 % *5*	9.44E-7 *13*
CE K	3109.6956 *7*	9E-6 % *9*	3E-7 *3*
CE L	3181.8391 *5*	1.8E-6 % *18*	6E-8 *6*
CE M	3193.8494 *5*	4E-7 % *4*	1.3E-8 *13*
CE N	3196.8064 *7*	1.1E-7 % *11*	3E-9 *3*
CE O	3197.625	2.1E-8 % *21*	7E-10 *7*
CE P	3197.698	2.2E-9 % *22*	7E-11 *7*

Gamma and X-ray radiation:

Energy (keV)	Intensity (%)	Dose (MeV/Bq-s)

XR l	10.6	2.75 % *12*	2.91E-4 *13*
XR kα2	72.805	2.01 % *6*	0.00146 *4*
XR kα1	74.969	3.35 % *9*	0.00251 *7*
XR kβ3	84.45	0.404 % *11*	3.42E-4 *10*
XR kβ1	84.938	0.776 % *22*	6.59E-4 *19*
XR kβ2	87.3	0.283 % *8*	2.47E-4 *7*
	211.40 *15*	0.180 % *10*	3.81E-4 *21*
	233.36 *15*	0.310 % *10*	7.23E-4 *23*
	252.61 *10*	0.780 % *20*	0.00197 *5*
	277.371 *5*	6.6 % *3*	0.0183 *8*
	485.95 *15*	0.049 % *4*	2.38E-4 *19*
	510.77 *10*	22.60 % *20*	0.1154 *10*
	583.187 *2*	85.0 % *3*	0.4957 *17*
	587.7	0.060 % *20*	3.5E-4 *12*
	650.1 *3*	0.050 % *20*	3.3E-4 *13*
	705.2 *3*	0.022 % *4*	1.6E-4 *3*
	722.04 *12*	0.24 % *4*	0.0017 *3*
	748.7 *2*	0.046 % *3*	3.44E-4 *22*
	763.13 *8*	1.79 % *3*	0.01366 *23*
	821.2 *2*	0.041 % *4*	3.4E-4 *3*
	860.557 *4*	12.50 % *10*	0.1076 *9*
	883.3 *2*	0.031 % *3*	2.7E-4 *3*
	927.6 *2*	0.125 % *11*	0.00116 *10*
	982.7 *2*	0.205 % *8*	0.00201 *8*
	1093.9 *2*	0.430 % *20*	0.00470 *22*
	1125.7 *4*	0.0050 % *20*	5.6E-5 *23*
	1160.8 *3*	0.011 % *3*	1.3E-4 *3*
	1185.2 *3*	0.017 % *5*	2.0E-4 *6*
	1282.8 *3*	0.052 % *5*	6.7E-4 *6*
	1381.1 *5*	0.007 % *3*	1.0E-4 *4*
	1647.5 *7*	0.0020 % *10*	3.3E-5 *16*
	1744.0 *7*	0.0020 % *10*	3.5E-5 *17*
	2614.511 *10*	99.754 % *4*	2.60808 *11*
	3197.7	0.004 % *4*	1.1E-4 *11*
	3475.1	0.0015 % *15*	5E-5 *5*
	3708.4	0.0020 % *20*	7E-5 *7*
	3960.9	0.0015 % *15*	6E-5 *6*

Gamma Coincidence Data:
For each gamma, the list of gammas in coincidence is given. If experimentally known, an estimate of the average time interval (in seconds) between both gammas is given

E(γ)	Coincidence
211.40	233.36 (1.00E-10), 277.371 (1.04E-10), 510.77 (1.00E-10), 583.187 (3.98E-10), 860.557 (1.04E-10), 1093.9 (1.00E-10), 2614.511 (4.14E-10), 3197.7 (3.98E-10), 3475.1 (1.04E-10), 3708.4 (1.00E-10)

233.36	211.40 (1.00E-10), 252.61 (1.00E-10), 277.371 (4.00E-12), 583.187 (2.98E-10), 587.7 (1.00E-10), 860.557 (4.00E-12), 2614.511 (3.14E-10), 3197.7 (2.98E-10), 3475.1 (4.00E-12)
252.61	233.36 (1.00E-10), 277.371 (1.04E-10), 510.77 (1.00E-10), 583.187 (3.98E-10), 860.557 (1.04E-10), 1093.9 (1.00E-10), 2614.511 (4.14E-10), 3197.7 (3.98E-10), 3475.1 (1.04E-10), 3708.4 (1.00E-10)
277.371	211.40 (1.04E-10), 233.36 (4.00E-12), 252.61 (1.04E-10), 485.95 (4.00E-12), 583.187 (2.94E-10), 587.7 (1.04E-10), 650.1 (4.00E-12), 705.2 (4.00E-12), 821.2 (4.00E-12), 883.3 (4.00E-12), 2614.511 (3.10E-10), 3197.7 (2.94E-10)
485.95	277.371 (4.00E-12), 583.187 (2.98E-10), 860.557 (4.00E-12), 2614.511 (3.14E-10), 3197.7 (2.98E-10), 3475.1 (4.00E-12)
510.77	211.40 (1.00E-10), 252.61 (1.00E-10), 583.187 (2.94E-10), 587.7 (1.00E-10), 2614.511 (3.10E-10), 3197.7 (2.94E-10)
583.187	211.40 (3.98E-10), 233.36 (2.98E-10), 252.61 (3.98E-10), 277.371 (2.94E-10), 485.95 (2.98E-10), 510.77 (2.94E-10), 587.7 (3.98E-10), 650.1 (2.98E-10), 705.2 (2.98E-10), 722.04 (2.94E-10), 748.7 (2.94E-10), 763.13 (2.94E-10), 821.2 (2.98E-10), 883.3 (2.98E-10), 927.6 (2.94E-10), 982.7 (2.94E-10), 1125.7 (2.94E-10), 1160.8 (2.94E-10), 1185.2 (2.94E-10), 1282.8 (2.94E-10), 2614.511 (1.66E-11)
587.7	233.36 (1.00E-10), 277.371 (1.04E-10), 510.77 (1.00E-10), 583.187 (3.98E-10), 860.557 (1.04E-10), 1093.9 (1.00E-10), 2614.511 (4.14E-10), 3197.7 (3.98E-10), 3475.1 (1.04E-10), 3708.4 (1.00E-10)
650.1	277.371 (4.00E-12), 583.187 (2.98E-10), 860.557 (4.00E-12), 2614.511 (3.14E-10), 3197.7 (2.98E-10), 3475.1 (4.00E-12)
705.2	277.371 (4.00E-12), 583.187 (2.98E-10), 860.557 (4.00E-12), 2614.511 (3.14E-10), 3197.7 (2.98E-10), 3475.1 (4.00E-12)
722.04	583.187 (2.94E-10), 2614.511 (3.10E-10), 3197.7 (2.94E-10)
748.7	583.187 (2.94E-10), 2614.511 (3.10E-10), 3197.7 (2.94E-10)
763.13	583.187 (2.94E-10), 2614.511 (3.10E-10), 3197.7 (2.94E-10)
821.2	277.371 (4.00E-12), 583.187 (2.98E-10), 860.557 (4.00E-12), 2614.511 (3.14E-10), 3197.7 (2.98E-10), 3475.1 (4.00E-12)
860.557	211.40 (1.04E-10), 233.36 (4.00E-12), 252.61 (1.04E-10), 485.95 (4.00E-12), 587.7 (1.04E-10), 650.1 (4.00E-12), 705.2 (4.00E-12), 821.2 (4.00E-12), 883.3 (4.00E-12), 2614.511 (1.66E-11)
883.3	277.371 (4.00E-12), 583.187 (2.98E-10), 860.557 (4.00E-12), 2614.511 (3.14E-10), 3197.7 (2.98E-10), 3475.1 (4.00E-12)
927.6	583.187 (2.94E-10), 2614.511 (3.10E-10), 3197.7 (2.94E-10)
982.7	583.187 (2.94E-10), 2614.511 (3.10E-10), 3197.7 (2.94E-10)
1093.9	211.40 (1.00E-10), 252.61 (1.00E-10), 587.7 (1.00E-10), 2614.511 (1.66E-11)
1125.7	583.187 (2.94E-10), 2614.511 (3.10E-10), 3197.7 (2.94E-10)
1160.8	583.187 (2.94E-10), 2614.511 (3.10E-10), 3197.7 (2.94E-10)
1185.2	583.187 (2.94E-10), 2614.511 (3.10E-10), 3197.7 (2.94E-10)
1282.8	583.187 (2.94E-10), 2614.511 (3.10E-10), 3197.7 (2.94E-10)
1381.1	2614.511 (1.66E-11)
1647.5	2614.511 (1.66E-11)
1744.0	2614.511 (1.66E-11)
2614.511	211.40 (4.14E-10), 233.36 (3.14E-10), 252.61 (4.14E-10), 277.371 (3.10E-10), 485.95 (3.14E-10), 510.77 (3.10E-10), 583.187 (1.66E-11), 587.7 (4.14E-10), 650.1 (3.14E-10), 705.2 (3.14E-10), 722.04 (3.10E-10), 748.7 (3.10E-10), 763.13 (3.10E-10),

	821.2 (3.14E-10), 860.557 (1.66E-11), 883.3 (3.14E-10), 927.6 (3.10E-10), 982.7 (3.10E-10), 1093.9 (1.66E-11), 1125.7 (3.10E-10), 1160.8 (3.10E-10), 1185.2 (3.10E-10), 1282.8 (3.10E-10), 1381.1 (1.66E-11), 1647.5 (1.66E-11), 1744.0 (1.66E-11)
3197.7	211.40 (3.98E-10), 233.36 (2.98E-10), 252.61 (3.98E-10), 277.371 (2.94E-10), 485.95 (2.98E-10), 510.77 (2.94E-10), 587.7 (3.98E-10), 650.1 (2.98E-10), 705.2 (2.98E-10), 722.04 (2.94E-10), 748.7 (2.94E-10), 763.13 (2.94E-10), 821.2 (2.98E-10), 883.3 (2.98E-10), 927.6 (2.94E-10), 982.7 (2.94E-10), 1125.7 (2.94E-10), 1160.8 (2.94E-10), 1185.2 (2.94E-10), 1282.8 (2.94E-10)
3475.1	211.40 (1.04E-10), 233.36 (4.00E-12), 252.61 (1.04E-10), 485.95 (4.00E-12), 587.7 (1.04E-10), 650.1 (4.00E-12), 705.2 (4.00E-12), 821.2 (4.00E-12), 883.3 (4.00E-12)
3708.4	211.40 (1.00E-10), 252.61 (1.00E-10), 587.7 (1.00E-10)

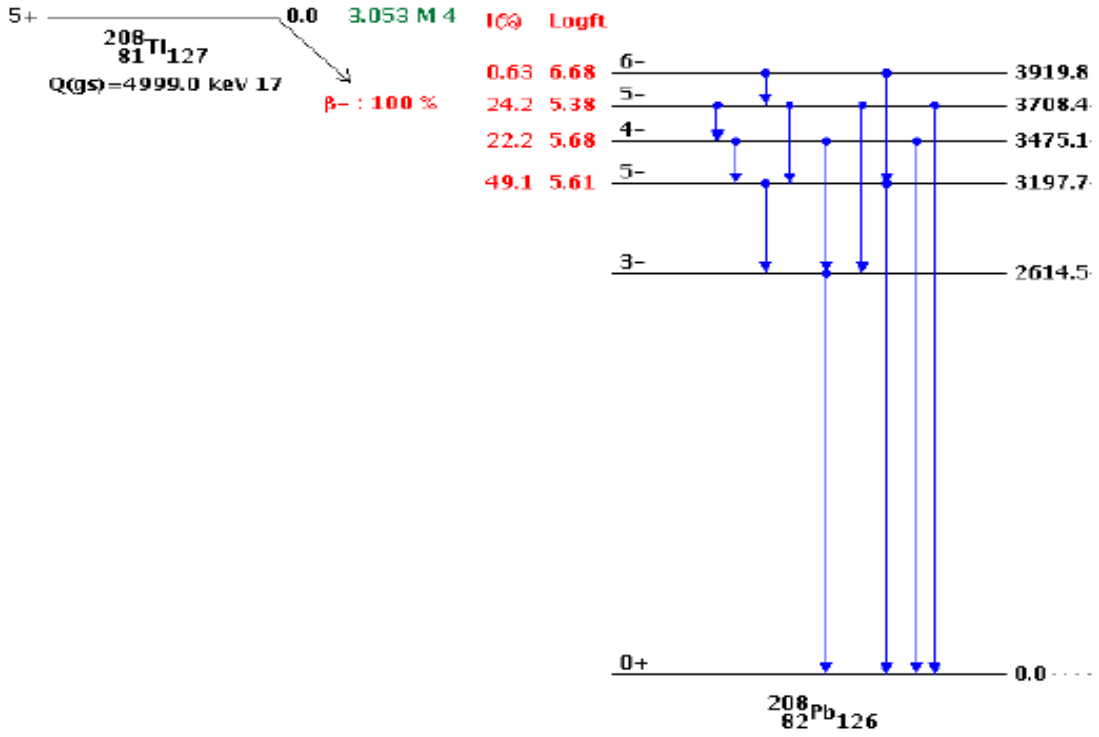

Figure 3.4 Decay Scheme of Thallium-208

We are now able to correctly say that when Uranium-232 is in equilibrium with Thallium-208, the number of nuclei in the Uranium-232 divided by the number of nuclei in Thallium-208 is equal to the decay rate of Uranium-232 divided by the decay rate of Thallium-208. Giving a decay rate ratio of the two isotopes, which is 3.16×10^{-8}. So the number of nuclei in Uranium-232

equals 4.3×10^{16} nuclei using the munber of Thallium-208 nuclei determined in the Appendix. This tells us that the true amount of Uranium-232 contaminant is 16.7 micrograms. Which also means the isotropic ratio of Uranium-232 to Uranium-233 is estimated to be about 4 ppm. This says our sample was an excellent one. In fact, it turns out to be better than any of the Uranium-233 targets in the U.S. Department of Energy inventory in regard to Uranium-232 contamination.

Since a better target than the one we have is not available, NRF measurements for Uranium-233 cannot be performed at the present time. In the future, if a pure Uranium-233 target becomes available, it might become possible to make such measurements.

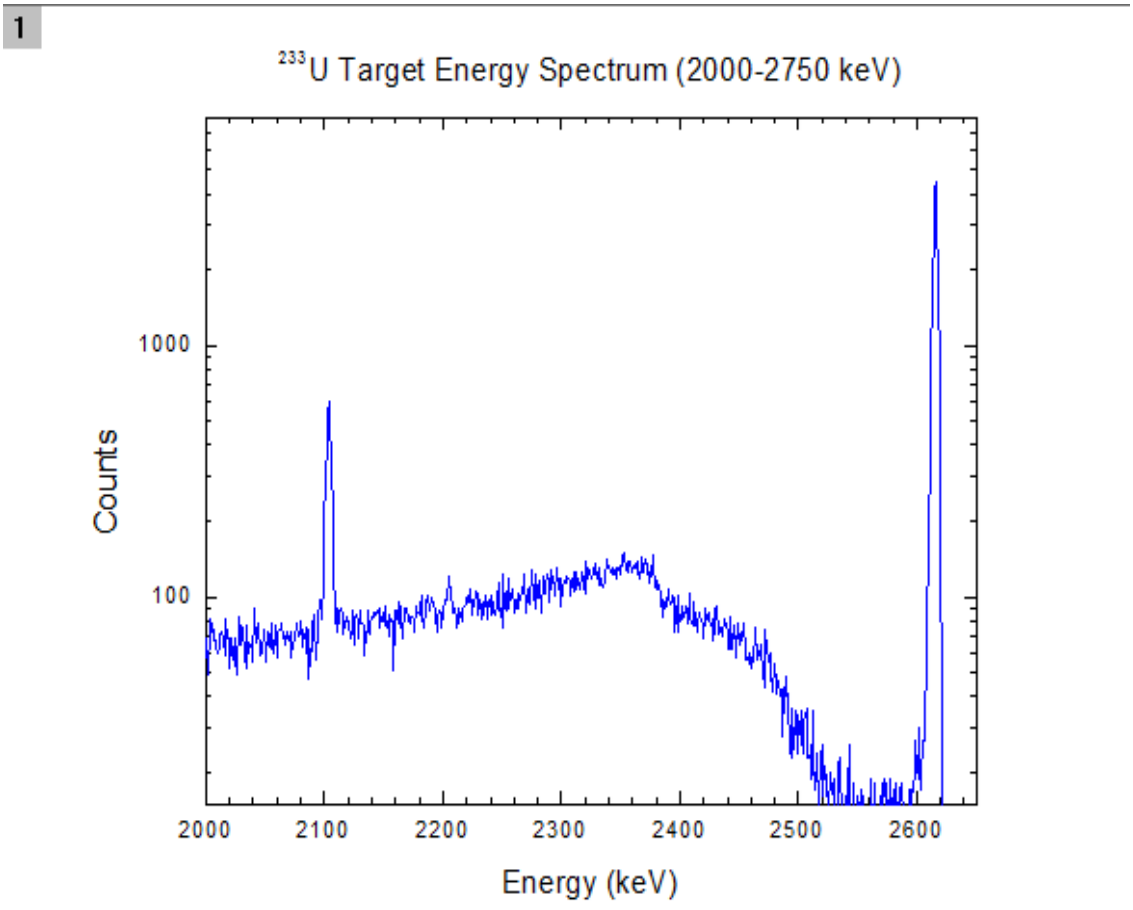

Figure 3.5. The gamma-ray line from the beta decay of Thallium-208.

The energy spectrum of the 2614 gamma-ray that comes from the daughter nuclei Thallium-208 in isotope Uranium-232 drowns out the activity of the Uranium-233, allowing it to be the best target available. This happens 99.754% of the time, which is stated in Table 3.1 of the characteristics of Thallium-208 above. The rest of the data collected is located in a chart in the appendix of this thesis.

CHAPTER 4

Nuclear Database

As stated before the Domestic Nuclear Detection Office of the Department of Homeland Security is interested in knowing the transition of gamma-rays through matter. A comprehensive database that all researchers and scientists can access the features was recommended. The database will be accessible online from the TUNL website and will have the following features;

1. Comprehensive non-evaluate database that includes cross sections, γ-ray transition rates and electromagnetic multi-polarity of transitions. Although the data are not evaluated, issues with data sets will be noted, e.g., published comments or errata that provide corrections or raise concerns about the data will be noted. Also, inconsistencies in tabulated values within a publication may be noted as well.
2. Data retrievable in a comma delimited format.
3. Publications of original work available via linked files (depending on agreements with scientific and engineering journals).
4. Intuitive user interface.
5. Browse and search capabilities.

The database will be one that can be changed and new information on (γ, γ') reactions can put into the database. A link from the Triangle Universities Nuclear Laboratory web page will be where you can access the database. The start of the database with the nuclear information looks like this:

Table 4.1 Brief look of the Nuclear Database

Iso-tope	Transition E_γ (keV)	Is (eV•b)	$\mathbf{J_i^\Pi \rightarrow J_f^\Pi}$	Γ_0^2/Γ (meV)	R_{exp}	Γ_0 (meV)	B(M1) ↑(μ_N^2)	B(E1) (e^2fm^2)	Ref.	Notes
^{1}H										No (g,g) reaction

^{6}Li	219		3^{+} ; 1^{+}						1	
^{7}Li	480		$(1/2)^{-}$;$(3/2)^{-}$						1	
^{9}Be										No (g,g) reaction
^{11}B										No (g,g) reaction
^{12}C										No (g,g) reaction
^{13}C	3089.44+/-0.02			424 +/- 41					17	
^{15}N										No (g,g) reaction
^{19}F	3906+/-6		$(3/2)^{+}$							
^{22}Ne	5326.2 +/- 1.3	0.10 +/- 0.04				250 +/- 0.10	0.15 +/-0.06		13,14	
^{23}Na	2985 +/-6		1^{+}			1120			15	
^{24}Mg	1368,59(4)		2^{+}	1,08(13)					Endt et van der Leun	
^{25}Mg										No (g,g) reaction
^{26}Mg	8227 +/- 2		$(1,2^{+})$			2300			13	
^{27}Al	2211		$(7/2)^{+}$	0,186(13)			0.14		2,15	
^{28}Si	10596 +/- 2		1^{+}			1.3 +/- 0.5			13	
^{31}P	3133 +/-5		$(1/2)^{+}$						15,16	
^{31}S										No (g,g) reaction
^{32}S	2230.57		2^{+}			2230.49			3	
^{34}S	7220 +/- 0.002	0.204 +/- 0.061	$(1),2^{+}$			0.92 +/- 0.28	-0.212			
^{35}Cl	2693.6 +/-0.1			12 +/- 3					15,16,17	
^{39}K										No (g,g) reaction
^{40}Ar	4768 +/- 1		1-						5	
^{40}K										No (g,g) reaction
^{40}Ca	3904.0(1)		2^{+}			15.7(43)		107.6(292)	4	
^{42}Ca										No (g,g) reaction
^{44}Ca	3661.3(2)		1^{-};1^{+}				3.16(76)	0.29(7)	6	
^{45}Sc	720(1)		$(5/2)^{-}$	1.58(16)		2.11(			7	
^{46}Ti										No (g,g) reaction
^{47}Ti										No (g,g) reaction
^{48}Ca	3831.5(2)		2^{+}			0.0000109(7)		96.8(105)	4	
^{48}Ti	3700 +/- 1		1^{+}	10 +/-1		20.4 +/- 2.3		1.2 +/-0.1	18	
^{49}Ti										No (g,g) reaction
^{50}Ti										No (g,g) reaction
^{50}Cr	3627.8		1^{+}				0.99(12)		9	
^{51}V	929.5(3)		$(3/2)^{-}$						8	
^{51}Cr										No (g,g) reaction
^{52}Cr	1434.1		2^{+}						9	
^{53}Cr	3180.8		$(3/2)^{-}$				0.06(1)		9	
^{54}Fe										No (g,g) reaction

^{55}Mn	7491		(3/2)						12	
^{56}Fe	3448.8+/-1.5	60+/-3	1	77+/-12		78+/-5		0.494+/-0.032	11	
^{57}Fe										No (g,g) reaction
^{57}Co										No (g,g) reaction
^{57}Ni										No (g,g) reaction
^{58}Ni	2014.9+/-0.4	23+/-3				7.9+/-1.1			10	
^{59}Co	1187		$(7/2)^-$	6.8			7.5		19,20	
^{60}Ni	1333								21	
^{61}Ni										No (g,g) reaction
^{62}Ni	1173		2^+						22	
^{63}Cu	1414		$(5/2)^-$	1.6			1.1		20	
^{64}Zn	3366		1			8.2+/-1.3			24	
^{65}Cu	1481.7+/-0.5		$7/2^-$	1.95(2)		1.15(12)			23	
^{66}Zn	3381		1			16+/-3			25	
^{67}Zn										No (g,g) reaction
^{68}Zn	3346		1			42+/-7				
^{69}Ga	872		$(5/2)^-$	1.1			0.8		27	
^{70}Ge	3240.4(4)	3.3+/-0.6	1^+	3.0+/-0.6		9.1+/-2.6	0.07+/-0.02		26	
^{71}Ga										No (g,g) reaction
^{72}Ge	2116.9(4)	2.7+/-0.3	1	1.1+/-0.2		1.2+/-0.6	0.03	0.33	26	
^{73}Ge										No (g,g) reaction
^{74}Ge	2403.5(5)	0.4+/-0.1	1	0.4+/-0.1		0.4+/-0.1	0.01	0.11	26	
^{75}As	7646		$(1/2)^-$			0.041+/-0.011	1.7		28	
^{76}Ge	2919.8(2)	2.1+/-0.8	1	1.5+/-0.6		1.5+/-0.6	0.02	0.18	26	
^{76}Se										No (g,g) reaction
^{77}Se										No (g,g) reaction
^{79}Br										No (g,g) reaction
^{80}Se	7820		1			0.030+/-0.007			29,30	
^{86}Sr	7820		1			0.030+/-0.015			30	
^{88}Sr	1835.9(1)	206(19)	2^+	60(6)					31	
^{88}Y										No (g,g) reaction
^{89}Y	4617.0(5)	4(1)		22(4)			0.020(4)	0.22(4)	32	
^{90}Zr	2186			4.89+/-0.28		4.89+/-0.28			33	
^{91}Zr	1205		$(1/2)^+$						34	
^{92}Zr										No (g,g) reaction
^{92}Mo	1509.8(1)		$2^+;0^+$						35	
^{93} Nb	744.2(1)	5.27(52)	$(7/2)^+;(9/2)^+$						36	
^{94}Mo	871.09(10)		$2^+;0^+$						37	
^{95}Mo										No (g,g) reaction

^{96}Mo										No (g,g) reaction
^{96}Ru	3154.2	95.2(30)	$1^+;0^+$						38	
^{98}Mo	3257.8(1)	4.5(4)	$1;0^+$				31(3)	0.34(3)	35	
^{98}Tc										No (g,g) reaction
^{99}Mo										No (g,g) reaction
^{100}Mo	2633.3(1)	1.5(3)	$1;0^+$				13(3)	0.14(3)	35	
^{100}Tc										No (g,g) reaction
^{103}Rh	1277	2.31(24)	$(3/2)^-;(5/2)^-$				0.0541(55)	0.599(61)	39	
^{105}Pd										No (g,g) reaction
^{106}Pd										No (g,g) reaction
^{107}Ag										No (g,g) reaction
^{108}Rh										No (g,g) reaction
^{108}Cd	1446.6	8.4(5)	$1^+;2^+$		19(3)		0.06(1)		40	
^{109}Ag										No (g,g) reaction
^{110}Cd	2650	25.1(6)	1^-			15.3(4)		2.35(5)	41	
^{111}Cd	2197	3.7(4)				4.59(22)	0.037(4)	0.41(5)	41	
^{112}Cd	2418	0.7(1)	$(1,2^+)$			0.34(7)	0.006(1)	0.07(1)	41	
^{113}Cd										No (g,g) reaction
^{113}In										No (g,g) reaction
^{114}Cd	2396	1.4(4)	1^-			0.7(2)		0.14(4)	41	
^{115}In										No (g,g) reaction
^{116}Cd	2478	18.2(11)	1^-			9.7(6)		1.82(11)	41	
^{116}Sn	4199.8	48(4)	1	73(6)		73(6)			42	
^{117}Sn	1147.2 (4)	2.31 (40)		1.26 (22)				0.398 (68)	43	
^{118}Sn										No (g,g) reaction
^{121}Sb	507		$(3/2)^-$	0.11(5)		0.12(6)			44	
^{122}Sn										No (g,g) reaction
^{122}Te	2592.3(2)	32(4)					92	1.01	45	
^{123}Sb	1032(1)		$(9/2)^+$	3.0(3)		3.0(3)			44	
^{124}Sn	4219.1(6)	22.6(24)	1	34.9 (37)		34.9 (37)			42	
^{124}Te	2812.5(2)	12.7(14)					0.37	34	45	
^{124}Xe	2182	18.7(13)	2^+		0.41 (7)	9.6(6)	0.239(15)	2.64(17)	46	
^{126}Xe	2359	9.4(7)	2^+		1.48 (14)	8.4(5)	0.166(10)	1.84(12)	46	
^{126}Te										No (g,g) reaction
^{127}I										No (g,g) reaction
^{128}Te										No (g,g) reaction
^{130}Te	2688.4(2)	8.0(10)					0.24	22	45	
^{130}Xe	2313	2.5(3)	2^+			1.14(16)	0.024(3)	0.264(36)	46	

^{131}Xe	1665	2.7(7)				1.93(52)	0.108(29)	1.20(32)	46	
^{132}Xe	2383	0.8(2)	2^+			0.40(12)	0.008(2)	0.085(25)	46	
^{133}Cs	2156	1.11+/-0.18				1.34+/-0.22			47	
^{134}Ba	2311	3.2+/-0.9	1			1.5+/-0.4	0.031+/-0.009		48	
^{135}Ba	980	9.01(64)				2.78(51)	0.255(47)		48	
^{136}Ba	2129	4.25(0.24)		1.00(6)		3.13(22)			48	
^{137}Ba	1294	11.72(59)				5.10(26)	0.204(10)		48	
^{138}Ba	1436	23.1(25)		2.48(27)		2.48(27)			48	
^{139}La										No (g,g) reaction
^{140}Ce	3643.8(6)		1^-	367 (56)				21.7(33)	50	
^{141}Pr										No (g,g) reaction
^{142}Ce	2187		$1^-;0^+$					3.62(12)	49	
^{142}Nd	3424.2(5)		1	295(44)				21.1(32)	50	
^{143}Nd	1407	20.7+/-6.7	$(9/2)^-$			8.6+/-2.8			51	
^{144}Nd	2072	5.44+/-	1^+			2.03+/-0.23	0.059+/-0.007		52	
^{144}Sm	3225.7		1	289(44)				24.8(38)	50	
^{146}Nd	1377	16.6+/-4.9	1^-		2.29 +/- 0.56	4.6+/-1.4			53	
^{148}Nd	1023	32.3+/-13.4	1^-		2.31 +/- 0.86	5.3+/-2.4			53	
^{148}Sm	1454.2(5)	3.61(37)	2^+			0.796(82)	0.0147(19)		54	
^{149}Sm										No (g,g) reaction
^{150}Nd	853	23.5+/-9.7	1^-		1.99 +/- 0.30	3.3+/-1.4		16.1+/-6.3	53	
^{150}Sm	2551.3		2^+			4.2(1.3)		0.7(2)	55	
^{151}Eu	889	3.80(63)	$5/2^-$			0.78(13)	0.096(16)		57	
^{152}Sm	2410.6		2^+			4.7(1.3)		0.9(2)	55	
^{153}Eu	1156	3.70(68)	$5/2^-$			1.29(24)	0.072(13)		57	
^{154}Sm	1972.6		2^+			4.4(9)	0.15(8)		55	
^{155}Gd	1675	7.3+/-0.9				5.3+/-0.6	0.097+/-0.011		56	
^{156}Gd	2027		1^+	3.9+/-1.2	0.25 +/- 0.24	5.0+/-1.8	0.16+/-0.05		58	
^{157}Gd	1956	2.55+/-0.39					0.029+/-0.004		59	
^{158}Gd	2268		1^+	6.9+/-1.2	0.46 +/- 0.12	10.2+/-1.9			58	
^{159}Tb	1254	35.0+/-9.0				24.0+/-5.0	1.100+/-0.200		56	
^{160}Gd	2348		1^+	8.3+/-1.5	0.52 +/- 0.09	12.8+/-2.4			58	
^{160}Dy	2822		1	59.3+/-6.6		94+/-11	1.09+/-0.13		59	
^{161}Dy										No (g,g) reaction
^{162}Dy	2395	36.3+/-1.9	1^+		0.57+/-0.03		0.52+/-0.03		59	

^{163}Dy	1542	1.62(27)				1.00(17)	0.024(4)		57	
^{164}Dy	1675	44.69+/-4.23	1^-		1.83 +/- 0.24	28.3+/-3.5		17.24+/-2.13	59	
^{164}Er	1387	47.1+/-4.6	1		2.17 +/- 0.26	21.7+/-3.5		23.31+/-3.76	60	
^{165}Ho	1381	6.67(65)				3.31(32)	0.109(11)		57	
^{166}Er	1663	63.6+/-7.0	1^-		1.74 +/- 0.07	38.1+/-4.7		23.74+/-2.93	60	
^{167}Er										No (g,g) reaction
^{168}Er	1786	58.6+/-5.6	1^-		1.91 +/- 0.05	44.5+/-5.0		22.38+/-2.51	60	
^{169}Tm	1510.6(4)	9.3(22)					0.139(32)	1.54(35)	61	
^{170}Er	1825	41.7+/-6.5	1^-		1.87 +/- 0.09	31.8+/-5.5		14.99+/-2.59	60	
^{171}Yb										No (g,g) reaction
^{172}Yb	1599			5.8+/-2.1		15.3+/-4.6		10.7+/-3.2	62	
^{174}Yb	1711			10.9+/-2.9		25.5+/-5.8		14.6+/-3.39	62	
^{175}Lu	1545	19.2(8)			0.276(40)				63	
^{176}Yb	2163			14.6+/-5.1		24.0+/-6.7	0.62+/-0.17	6.8+/-1.9	62	
^{176}Lu										No (g,g) reaction
^{176}Hf	1643	13.0(9)	1^-		1.72 (16)	7.5(4)		4.82(23)	64	
^{177}Hf										No (g,g) reaction
^{178}Hf	1174.6	7.9+/-3.1	2^+			1.00+/-0.41			64	
^{179}Hf										No (g,g) reaction
^{180}Hf	2120.1	2.6+/-1.3	1			1.00+/-0.49	0.027+/-0.013	0.30+/-0.15	64	
^{180}Ta										No (g,g) reaction
^{180}W										No (g,g) reaction
^{181}Ta	1866	5.43+/-0.86				4.92+/-0.78			65	
^{182}W	2382	21.6+/-2.5	1		1.42 +/- 0.20	1.76+/-0.25	0.46+/-0.06	5.04+/-0.68	66	
^{183}W										No (g,g) reaction
^{184}W	2056	9.0+/-0.7	1^-		1.55 +/- 0.25	0.95+/-0.09		2.7+/-0.3	66	
^{185}Re										No (g,g) reaction
^{186}W	2557	8.8+/-0.8	1		0.43 +/- 0.10	0.41+/-0.05	0.11+/-0.01	1.17+/-0.13	66	
^{187}Re	512		$(1/2)^+;(5/2)^+$						67	
^{188}Os										No (g,g) reaction
^{189}Os										No (g,g) reaction
^{190}Os	1115.5	8.5(15)					0.172(29)	1.90(32)	68	

^{191}Ir										No (g,g) reaction
^{192}Os	2391.2	8.86(83)					0.0835(78)	0.920(85)	68	
^{193}Ir										No (g,g) reaction
^{194}Pt	2517.2(4)	6.0(8)	1				0.054(7)		69	
^{195}Pt										No (g,g) reaction
^{196}Pt	2246.3	4.7(15)	1^{+}			2.7(9)	0.061(20)		69	
^{196}Au										No (g,g) reaction
^{197}Au										No (g,g) reaction
^{198}Hg										No (g,g) reaction
^{199}Hg										No (g,g) reaction
^{201}Hg										No (g,g) reaction
^{202}Hg										No (g,g) reaction
^{203}Tl	1411		$(1/2)^{+}$						70	
^{204}Pb										No (g,g) reaction
^{205}Tl										No (g,g) reaction
^{206}Pb	4974					0.0008			70,71,72	
^{207}Pb	4847					13			70,71,72	
^{208}Pb	4085					0.51			70,71,72	
^{209}Bi	4228					3			73	
^{232}Th	2043.7(3)	46.3(45)		16.8(16)	0.62 (9)		1.34(13)		73,74 ,75	
^{235}U	1656.4(7)	3.0(11)	$(7/2)^{-}$	2.1(8)	1		20		75,76, 77	
^{236}U	1791.3		1	5.7(+/-)0.7	0.41 (+/-)0.09	8.3(+/-)1.1	0.38(+/-)1.1		78	
^{238}U	1996.7(3)	7.0(8)	1-	2.8(3)	0.19 (2)	48.6(+/-)2.7	1.48(+/-)0.09	1.2(2)	79, 80	

CHAPTER 5

Summary

Based on everything that was gathered from the assay of Uranium-233, we have a sample that is about 37 years old with 4 ppm of Uranium-232. All experiments were done at Duke University with the faculty and staff on hand there. The Uranium-233 assay was solely the author of this project's task to complete. Its information gathered is a part of a larger experiment that will be continued well after this work is completed.

Given that it is unlikely that there is another Uranium-233 target with less Uranium-232 contaminant, Uranium-233 targets are unsuitable for use in Nuclear Resonance Fluorescence measurements. This concludes the work.

References

[1] http://www.studyphysics.ca/2007/30/08_atomic/43_decay.pdf

[2] http://tb014.k12.sd.us/Chemistry/Neclear%20Reactions/types3.html

[3] http://www.gcsescience.com/prad10-gamma-nuclear-equations.htm

[4] J. Margraf et al., Phys. Rev. C http://dx.doi.org/10.1103/PhysRevC.42.771 **42**, 771(1990).

[5] C. P. J. Barty and F. V. Hartemann, Lawrence Livermore Laboratory Report No. UCRL-TR-206825, 2004 (unpublished).

[6] D. Slaughter et al., Lawrence Livermore Laboratory Report No. UCRL-ID-155315, 2003 (unpublished).

[7] COMDEX FALL November 18, 1981 Las Vegas, NV, "Tecmar shows 20 IBM PC option card.. LabMaster,LabTender,DADIO,DeviceTender,IEEE-488.."

[8] PC Magazine Vol1 No.1, "Taking the Measure" by David Bunnell, "Tecmar deployed 20 option cards for the IBM PC"

[9] Bremsstrahlung radiation" is "braking radiation", but "acceleration" is being used here in the specific sense of the *deflection* of an electron from its course: Serway, Raymond A; et al (2009). *College Physics*. Belmont, CA: Brooks Cole. p. 876. ISBN 978-0-03-023798-0.

[10] Knoll, G.F. (1999). *Radiation Detection and Measurement, 3rd edition*. Wiley. ISBN 978-0-471-07338-3. p365

[11] http://www.tunl.duke.edu/groups/nnsa/nrf.html#intro

Appendix

Table A-1 Isotopes

Isotope	213Bi	208Tl	208Tl	208Tl	221Fr*	229Th	212Bi	212Bi**	212Pb***
Half-Life (s.)	2735.4	183.18	183.18	183.18	294	2.31628E+11	3633	3633	38304
Uncertainty	3.6	0.24	0.24	0.24	12	5049105408	3.6	3.6	36
BR	0.2594	0.85	0.125	0.99754	0.114	0.0299	0.0667	0.0147	0.436
Uncertainty	0.0015	0.003	0.001	0.00004	0.003	0.003026549	0.0009	0.0003	0.005
Tag	233U	232U	232U	232U	233U	233U	232U	232U	232U
Meas. E(MeV)	0.439719	0.5823699	0.859457	2.614584	0.217381	0.210055		1.619849	0.2381354
Actual E(MeV)	0.44045	0.583187	0.860557	2.614511	0.21812	0.21015	0.72733	1.6205	0.238632
FWHM	3.026	3.118	3.242	4.177	3.013	3.24		3.73	3.221
Uncertainty	0.017	0.014	0.042	0.03	0.041	0.16		0.13	0.012
Area	29047	45072	5420	20732	17077	4558		1244	93250
Uncertainty	184	218	80	145	226	209		43	346
Atten. w/ Coh. Scatt.	0.2271	0.1466	0.09025	0.04459	0.9477	1.033	0.1097	0.05307	0.7726
Atten. w/o Coh. Scatt.	0.2114	0.1374	0.08587	0.0441	0.8907	0.9717	0.1036	0.0518	0.7241
w/ Coh. Trans. Coeff.	1.239913767	0.800402282	0.492744243	0.243451144	5.174224029	5.63994241	0.598936769	0.289749994	4.218218302
w/o Coh. Trans. Coeff.	1.154195378	0.750172398	0.46883045	0.240775857	4.863017139	5.305258509	0.565632172	0.282816086	3.953419457
w/ Coh. Trans. Frac.	0.950524865	0.967679145	0.979934957	0.990018531	0.813852711	0.7994965	0.975681321	0.988135354	0.844458361
w/o Coh. Trans. Frac.	0.953838232	0.969666014	0.980896267	0.990127493	0.823645381	0.809777599	0.977012701	0.988417081	0.853215172
Efficiency (122.5 cm)	5.98397E-05	5.15317E-05	4.08583E-05	1.7954E-05	8.14331E-05	8.25553E-05	4.53312E-05	2.63303E-05	7.87E-05
Frac. Uncertainty	0.041062524	0.037389295	0.029500652	0.098778869	0.040891308	0.041055506	0.032819317	0.049432802	0.040805283
Scaled Eff. (245 cm)	1.59184E-05	1.34846E-05	1.05692E-05	4.60104E-06	2.50869E-05	2.58681E-05	1.17729E-05	6.7593E-06	2.34046E-05
Frac. Uncertainty	0.044730546	0.041384178	0.034423528	0.100359134	0.044573421	0.044724103	0.037306814	0.052519451	0.044494516

Table A-2 Characteristics of the isotopes.

Live Time:	1447.033333
Real Time:	1536.6
Distance (cm):*	245
Density Est. (g/cm^3):	5.45977
Target Half-Thickness (cm):	0.08255
Solid Angle Point Source (sr):	0.0021400
Uncertainty:	0.0000171
Solid Angle Target (sr):	0.0005430

Uncertainty:	0.0000086
233U Half-Life (s):	5.024E+12
Uncertainty (s):	6.311E+09
232U Half-Life (s):	2.174E+09
Uncertainty (s):	1.262E+07
233U Activity (Bq):	1.426E+09
233U Mass (g)	4.000E+00

Table A-3 Energy transitions, cross section and activity from analysis of the isotopes

Isotope	**Tag**	**E(MeV)**	**Area**	**Uncertainty**	**Area (Eff. Corr.)**	**Frac. Uncertainty**	**Activity (Bq)**	**Implied Source Age (yr)******	**232U (Bq) – 36.25**	**232U (mCi)**	**232U Mass (g)**	**PPM 232U**
213Bi	233U	0.44045	29047	184	1824738778	0.045176857	4.861E+06	36.25				
208Tl	232U	0.583187	45072	218	3342475276	0.04166586	2.718E+06		10440000	0.282162162	1.26181E-05	3.168E-06
208Tl	232U	0.860557	5420	80	512809475.7	0.037454522	2.835E+06		10887000	0.294243243	1.31584E-05	3.304E-06
208Tl	232U	2.614511	20732	145	4505938716	0.100602545	3.122E+06		11990000	0.324054054	1.44915E-05	3.639E-06
221Fr*	233U	0.21812	17077	226	680714368.2	0.046496594	4.126E+06	30.78				
229^{Th}	233U	0.21015	4558	209	176201318.5	0.064052976	4.072E+06	30.28				
212Bi	232U	0.72733			0		0.000E+00					
212Bi**	232U	1.6205	1244	43	184042644	0.062873646	8.652E+06		11938000	0.322648649	1.44287E-05	3.623E-06
212Pb***	232U	0.238632	93250	346	3984251051	0.044648958	6.315E+06		8713000	0.235486486	1.05308E-05	2.644E-06
							Average	32.44	11313750	0.305777027	1.36742E-05	3.433E-06
							Age:					